Demystifying strange metal and violation of Luttinger theorem in a doped Mott insulator

Wei-Wei Yang,¹ Yin Zhong,^{1,*} and Hong-Gang Luo^{1,2}

¹School of Physical Science and Technology & Key Laboratory for Magnetism and Magnetic Materials of the MoE, Lanzhou University, Lanzhou 730000, People Republic of China ²Beijing Computational Science Research Center, Beijing 100084, China (Dated: June 11, 2021)

Metallic states coined strange metal (SM), with robust linear-T resistivity, have been widely observed in many quantum materials under strong electron correlation, ranging from high- T_c cuprate superconductor, organic superconductor to twisted multilayer graphene and MoTe₂/WSe₂ superlattice. Despite decades of intensive studies, the mystery of strange metal still defies any sensible theoretical explanation and has been the key puzzle in modern condensed matter physics. Here, we solve a doped Mott insulator model, which unambiguously exhibits SM phenomena accompanied with quantum critical scaling in observables, e.g. resistivity, susceptibility and specific heat. Closer look at SM reveals the breakdown of Landau's Fermi liquid without any symmetry-breaking, i.e. the violation of Luttinger theorem. Examining electron's self-energy extracted from numerical simulation provides the explanation on the origin of linear-T resistivity and suggests that the long-overlooked static fluctuations in literature play an essential role in non-Fermi liquid behaviors in correlated electron systems.

Metallic quantum states deviated from the prediction of Landau Fermi liquid (FL) theory have been widely observed in many quantum materials since the discovery of high- T_c cuprate superconductor. Among these non-Fermi liquid (NFL) states, the strange metal (SM) with robust linear-T resistivity stands out due to its ubiquitousness in correlated superconductors, heavy fermion compounds and recently uncovered twisted multilayer graphene. Since in many cases of copper oxides the superconductivity emerges directly as an instability of the SM phase, it is believed that understanding the nature of SM should be the key step to solve the high- T_c problem in cuprate and to establish the general framework for NFL phenomena $^{1-13}$.

To attack SM, plenty of intriguing theoretical proposals are created wherein the aspect of doped Mott insulator (MI) due to Phil Anderson suggests a fruitful pathway culminated in classic SU(2) gauge field theory. Unfortunately, the strong coupling nature of gauge theory hinders the correct solution of doped MI though the perturbative calculation does predict a linear-T behavior in resistivity $^{14-16}$. Alternatively, recent progress on doped Hubbard model armed with state of art dynamic-mean-field-theory (DMFT) revisits the issue of doped MI, concluding that the elusive SM behaviors are caused by the doping-driven Mott quantum criticality 17,18 . More recent quantum Monte Carlo (QMC) study confirms SM at high-T regime and suggests unambiguously the breakdown of Landau FL by the violation of Luttinger theorem $^{19-21}$.

However, we have to emphasize that the mystery of SM has not been demystified due to the following reasons:(1) Since non-local spatial fluctuation which is important in quantum criticality has been largely neglected in DMFT, the Mott criticality driven SM phenomena may be fragile when spatial fluctuation are recovered; (2) The QMC study only establishes the existence of SM at rather high-*T* while the fate of SM at physically more relevant low-*T* regime (relevant to realistic experiments) has not been clarified due to the notorious fermions minus-sign problem for QMC; (3) Only Hubbard model has been carefully examined, but models beyond Hubbard are crucial to understand many-bands systems like heavy fermion compounds^{22–24}; (4) Finally, no analytic or semi-analytic re-

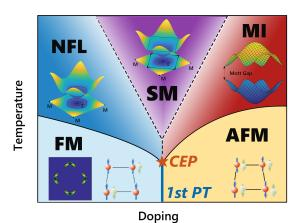


FIG. 1. Schematic phase diagram of the hole-doped Ising-Kondo lattice (IKL) model. The low temperature regime is divided into an antiferromagnetic insulator (AFMI) and a ferromagnetic metal (FMM) by a first-order transition, which transforms to a weak first-order transition and finally ends at the critical end point (CEP). At high temperature above CEP, a quantum critical region (QCR) is induced by doping-driven Mott insulator-metal transition, which displays the strange metal (SM) behaviors. Out of QCR, there exists a Mott insulator (MI) at lower doping and a non-Fermi liquid (NFL) at a higher doping. Inset in MI shows two-band structure active at strong coupling while only lower band is depicted for SM and NFL.

sults are available in those numerical simulations, which are just black boxes if one cannot extract analytic formalism.

Motivated by aforementioned important progresses and unsolved issues, in this work we seek a clear and complete understanding about SM behaviors in doped MI with the help of an alternative model, which allows for nearly complete analytical and numerical treatment. Our departure is the doped Ising-Kondo lattice (IKL) model, which naturally mimics the strongly correlated f electron materials CeIrSn²⁵, TmB₄²⁶, hidden order compound URh₂Si₂²⁷ and at the same time could

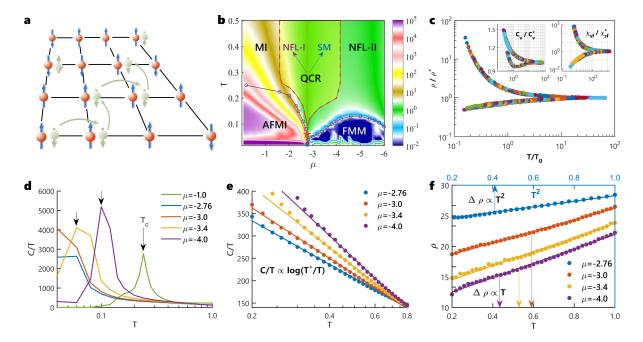


FIG. 2. Schematic picture, phase diagram of IKL and strange-metal behaviors in the QCR. a Schematic representation of the doped IKL. b Phase diagram of the doped IKL model on square lattice in $\mu-T$ plane with J=14. Rich quantum states include AFMI, FMM, MI, insulator-like non-Fermi liquid (NFL-I), SM, and the second non-Fermi liquid (NFL-II). The background is a color map of the resistivity. Thermal fluctuation driven magnetic-paramagnetic phase transition is denoted by the purple line with circle mark. The first-order phase transition at ground state is marked by a blue circle. The CEP is marked by a red pentagram. The QCR is delimited by the crossover temperature (red dashed line). c Unconventional quantum scaling behavior of resistivity in the QCR. Family of resistivity curves are calculated along lines parallel to the separatrix $\mu^*(T)$ and all can be rescaled in the formula $\rho(T, \delta \mu)/\rho^*(T) = f(T/T_0(\delta \mu))$. Inset plots the quantum scaling behavior of thermodynamic properties, i.e., heat capacity C_V of c electron and the susceptibility of f electron χ_{sf} . d-f Anomalous transport and thermodynamics in the SM. d Specific heat under different doping. The peak position corresponds to T_C of magnetic-paramagnetic phase transition. e The same plot of specific heat in paramagnetic region with the y-axis magnified. In SM, C(T)/T exhibits logarithm temperature dependence. The solid line is fitted by a $\log(T^*/T)$ function. f Resistivity under different doping. In the QCR $\rho(T)$ satisfies a power-law dependence of temperature ($\rho(T) = \rho_0 + AT^n$). With increasing doping, the resistivity changes from T^2 -dependent behavior ($\mu = -2.76$) to a linear-T dependence ($\mu = -3.0, -3.4, -4.0$), indicating the SM behavior.

be simulated by the unbiased Monte Carlo methods. In this solid platform, the competition between local and itinerant tendency involves non-trivial SM physics. The macroscopic anomalies include the robust nonsaturating, *T*-linear resistivity and the logarithmic temperature dependence of specific-heat coefficient. Such exotic SM behaviors beyond the quasiparticle paradigm turn to be intrinsically connected with the quantum criticality, which has also been observed in the vicinity of the quantum critical point (QCP) in various quantum critical heavy electron materials. The absence of quasiparticle picture is clearly indicated by a strong violation of Luttinger theorem throughout the phase diagram. Further study shows that the IKL model exhibits these SM characters as a direct consequence of a NFL like self-energy, which provides natural routes to linear resistivity in SM phase.

Results

Model and phase diagram.-We consider the IKL model on square lattice whose Hamiltonian is defined as

$$\hat{H} = -t \sum_{i,j\sigma} \hat{c}^{\dagger}_{i\sigma} \hat{c}_{j\sigma} + \frac{J}{2} \sum_{j\sigma} \hat{S}^{z}_{j\sigma} \hat{c}^{\dagger}_{j\sigma} \hat{c}_{j\sigma} - \mu \sum_{j\sigma} \hat{c}^{\dagger}_{j\sigma} \hat{c}_{j\sigma}, (1)$$

where $\hat{c}^{\dagger}_{j\sigma}(\hat{c}_{j\sigma})$ is c electron's creation (annihilation) operator

with spin $\sigma=\uparrow,\downarrow$ at site j. \hat{S}_j^z denotes the localized moment of f electron. t-term denotes the hopping integral and only nearest neighbor hoping is involved. The hole doping into the half-filled system $(\mu=0)$ is realized by tuning the chemical potential μ . J is the longitudinal Kondo coupling. Choosing eigenstates of \hat{S}_j^z as basis, Eq. (1) reduces into an effective free fermion model²⁸ under fixed background $\{q_j\}$, $(q_j=\pm 1, \hat{S}_j^z|q_j\rangle = \frac{q_j}{2}|q_j\rangle$) thus permits a straightforward classical (lattice) Monte Carlo simulation²⁹.

In IKL model, the competition between itinerant and local tendency leads to different magnetic order, and thus further conspire to construct rich quantum states, including antiferromagnetic insulator (AFMI), ferromagnetic metal (FMM) at low temperature and paramagnetic phases as MI, SM, NFL at high temperature³⁰. There exists a critical end point (CEP, see the red pentagram in Fig. 2b), below which a first-order phase transition separates the IKL system into AFMI and FMM. Above CEP, a QCR with unusual quantum scaling behavior is uncovered. Our main result about the doped IKL is summarized in the $\mu-T$ phase diagram (see Fig. 2b), where the color bar denotes resistivity scaled by the one in the separatrix line

(dotted line) of QCR³¹.

Strange metal and quantum critical scaling-The presence of SM state is ascertained by anomalous thermal and transport properties 5,6,32,33 . We plot the evolution of heat capacity C(T) and resistivity $\rho(T)$ with varying doping in Fig. 2d,e,f. In SM phase, the heat capacity coefficient C(T)/T increases with decreasing temperature, exhibiting an obvious dependence proportional to $\log(T^*/T)$ before approaching the magnetic phase transition, where T^* is the cut-off temperature. As to resistivity, an obvious linear-T dependence is revealed, which is nonsaturating with increasing temperature.

It has been suggested that it is the quantum critical physics who leads to both linear-T resistivity and high- T_c superconductivity. In most heavy fermion materials, the linear-T resistivity is observed when tuning some external parameters to create the QCP^{34–38}. In our model, even without the QCP, canonical signatures of quantum criticality are uncovered in a fan-like region together with the SM phase in various physical properties, including the resistivity, heat capacity and the magnetic susceptibility. In Fig. 2c we plot the unconventional quantum scaling behavior of these transport and thermodynamic observables 39. As a whole, resistivity in the QCR (see fig. 2f) demonstrates a power-law dependence of temperature, satisfying $\rho(T) = \rho_0 + AT^n$, and the *n* gradually changes from 2 to 1 as the crossover to SM is occurring. Detailed study indicates the resistivity of QCR satisfies the following quantum critical scaling

$$\rho(T, \delta \mu) = \rho^*(T) f(T/T_0(\delta \mu)), \tag{2}$$

where $T_0(\delta \mu) = c |\delta \mu|^{z\nu}$, $\delta \mu = \mu - \mu^*(T)$ and $\mu^*(T)$ is the critical 'zero field' trajectory corresponding to the 'separatrix' line⁴⁰. $\rho^*(T)$ is calculated for $\mu = \mu^*(T)$ and f(x) denotes the unknown scaling function. The resistivity on the separatrix is almost independent with temperature. Note that at high temperatures, the resistivity curves depend weakly on different parameter, while as temperature is reduced the critical line separates resistivity curves to two branches. Here, we refer the insulator-like branch to the first NFL state (NFL-I)⁴¹ and the metallic one to SM, respectively. The resistivity curves display the bifurcating characteristic. Crossing the center line, there is a change in trend with varying temperature. Both branches display the power-law scaling $T_0(\delta \mu) = c |\delta \mu|^{z\nu}$ with the same exponents zv = 1.25, and the $T_0(\delta \mu)$ vanishes as $\delta\mu \to 0$, indicating a quantum criticality instead of classical phase transition⁴².

Violation of Luttinger theorem.-Given the unconventional quantum criticality, it is natural to further confirm the quasiparticle properties of the exotic SM phase. To this aim, we examine the validity of Luttinger theorem in our model^{43–45}, which states that if Landau quasi-particle exists, the volume enclosed by Fermi surface is consistent with its density of particles. Such theorem has been proved originally by Luttinger in terms of perturbation theory⁴⁴, and later by Oshikawa's non-perturbation topological argument⁴⁵. It now has been accepted as a key feature of FL. Mathematically, Luttinger theorem means the Luttinger integral (IL) below must be equal to

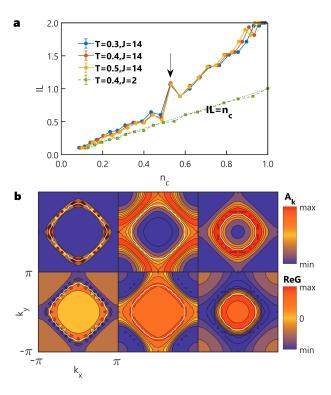


FIG. 3. **Violation of Luttinger theorem. a** Luttinger integral (IL) versus density of electron n_C . In FL (J=2), the electron density is in accordance with the Luttinger theorem. At strong coupling (J=14), IL strongly deviates from the density of electrons for most doping regime thus confirms their NFL nature. IL diverges close to the boundary of QCR. Divergence is indicated by the arrow. **b** Spectral function at Fermi energy $A_k(\omega=0)$ (upper panel) and real part of Green function at Fermi energy $ReG(k, \omega=0)$ (lower panel) in different high-temperature phases: FL (left panel, J=2, T=0.4, $\mu=-0.8$); SM $(J=14, T=0.4, \mu=-3.0, \text{middle panel})$; NFL-II $(J=14, T=0.4, \mu=-4.6, \text{right panel})$. Electron density is denoted by the size of the Fermi surface's volume in a free system (white circle). The maximum of spectral function corresponds to the Fermi surface under strong coupling.

density of particles (n_c)

$$IL = \sum_{\sigma} \int_{\theta(\text{Re}G(k,\omega=0))} \frac{d^d k}{(2\pi)^d}.$$
 (3)

However, we note the whole high temperature region of IKL violates the Luttinger theorem heavily. The strong violation of the Luttinger theorem is demonstrated in Fig. 3a, which is robust with arbitrary doping for the strong coupling (J=14, IL $\sim 2n_c$). It suggests a robust NFL-like nature for all paramagnetic phases in the phase diagram (see Fig. 2b), including SM. As a reference, we also show that the Luttinger theorem works well in the weak coupling case (J=2, IL $\sim n_c$), agreeing with its FL nature. Extra feature in Fig. 3a is that the IL shows incipient divergence around $n_c \sim 0.53$, which is close to the boundary of QCR.

The violation of Luttinger theorem could be characterized

clearly by c electron's single-particle spectral properties. As shown in Fig. 3b, c electron's spectral function $A_k(\omega = 0)$ and the real part of Green function $ReG(k, \omega = 0)$ at Fermi energy are carefully studied. We compare the Luttinger integral and electron density in FL (left panel), SM (middle panel) and NFL-II (right panel). According to Luttinger theorem, electron density can be denoted by the size of the Fermi surface's volume in the free system (white line). Figure 3b shows nicely and clearly the working of the Luttinger theorem for the FL. Under weak coupling the volume enclosed by the Fermi surface is consistent with the one in free system ($n_c = 0.36$). It suggests the presence of quasiparticle, since in this weak coupling situation the volume enclosed by the Fermi surface has not changed due to interaction. To the contrary, both the SM $(n_c = 0.67)$ and NFL-II $(n_c = 0.31)$ states display violation of Luttinger theorem, where the electron density is deviated from the volume enclosed by the Fermi surface, underlying the destruction of quasiparticle in the paramagnetic regime of the doped IKL.

Microscopic mechanism underlying SM behaviors.-Qualitatively, we have located the NFL nature of SM state by confirming the violation of Luttinger theorem. Next by extracting electron's self-energy $\Sigma(k,\omega)$ via Dyson equation, we can get more specific and concrete formula to describe these SM behaviors. We plot the real and imaginary parts of selfenergy at Fermi energy respectively (see Fig. 4a-f). The Fermi surface is demonstrated in Fig. 4a and the momentum is chosen along the doted line. In FL, the quasiparticle dominates the low-energy physics and it leads to a quadratic-k dependent behavior in imaginary part of self-energy around the Fermi energy due to the phase space effect. (As reference, we show the momentum dependence of FL (J = 2, T = 0.4) around Fermi surface in Fig. 4b. Its real part displays a linear dependence of k.) Intriguingly, it turns out a quite different rule is enforced in the paramagnetic region of the IKL. In SM $(J = 14, \mu =$ -3.0, T = 1.0) and NFL-II ($J = 14, \mu = -4.6, T = 1.0$), both real and imaginary parts demonstrate linear-k dependence $\text{Re}\Sigma(\omega=0) \sim k - k_{\text{F}}, \text{Im}\Sigma(\omega=0) \sim k - k_{\text{F}}.$

Since the famous marginal FL theory has provided a reasonable functional form of self-energy to phenomelogically describe the normal state of the optimal doped cuprates 35 , a natural question posed by these observations is whether some quantitative microscopic description responsible for these SM behaviors is also accessible for the IKL system. Inspired by the analytic Hubbard-I approximation, we note the frequency dependence of self-energy can be fitted with $\Sigma(\omega) \sim \frac{J^2/16}{\omega + \mu + i \Gamma}$, as shown in Fig. 4e,f 46 . Thus in NFL-II/SM, the self-energy at the Fermi energy is approximately given by

$$\Sigma(\mathbf{k},\omega) = a \frac{J^2/16}{\omega + \mu + i\Gamma} + b(\mathbf{k} - \mathbf{k}_{\rm F}), \tag{4}$$

where $k_{\rm F}$ is the Fermi momentum. Hitherto, several analytical approaches have been developed to study the source of linear-T behavior, where the power-law functional form of self-energy $(\Sigma(\omega) \approx |\omega|^a)$, where a < 1 is the main goal 47,48. However, the exact form of self-energy can only be revealed in some soluble models, such as the Sachdev-Ye-Kitaev (SYK) model 49,50

and the Hatsugai–Kohmoto (HK) model⁵¹. Equation. 4 extracted from the reliable Monte Carlo simulation provides a distinct functional form of self-energy which could also result in the linear-T resistivity.

To further confirm the connection between SM state and the nontrivial self-energy formula, next we try to reproduce the linear-T resistivity with Eq. 4. We note this self-energy is quite robust under varying temperature at the whole paramagnetic region, which suggests a robust two-peak spectral function and at the same time a T-independent scattering rate. Previous study on the Hubbard and SYK models states that the broadening of spectral function by a T-independent scattering rate contributes heavily to the T-linear resistivity 52 . Therefore, we expect the linear-T resistivity emerges in the SM phase can as well be attributed to the T-independent feature of this nontrivial self-energy Eq.4. With the optimal fitting coefficients 53 of Eq.4 we calculate the resistivity by the Kubo formula

$$\sigma_{DC} = 2\pi \int d\epsilon \phi(\epsilon) \int \frac{\beta d\omega A(\epsilon, \omega)^2}{4 \cosh^2(\beta \omega/2)}.$$
 (5)

As shown in Fig. 4g,h, a strictly linear-*T* dependence is demonstrated for all coupling strength, which is robust within a wide range of doping. Therefore, we conclude that our system accesses to robust linear-*T* resistivity with the self-energy in the form of Eq. 4.

What's more, since the doping level determines the main energy scale, it also plays a dominant role in the transport properties. Unexpectedly, at most parameter region the slope of linear-*T* resistivity is roughly proportional to the inverse of doping as shown in Fig. 4h, which could be fitted by

$$\rho(T, n_c) \approx \rho_0 [n_c + \frac{C}{n_c} T]. \tag{6}$$

Importantly, such behavior is agreeing with recent experiments for cuprates, heavy fermion and quantum critical metal $Sr_3Ru_2O_7^{6,10}$ and also the magic-angle graphene⁵⁴. This consistency underlines the basic physics captured by the IKL has shown the common trend of generic strongly correlated electron systems.

Discussion and conclusion.-We remark that a similar phase diagram like Fig. 2b has been reported in the Hubbard model with the DMFT approximation 17,18 . Comparing the anomalous phenomena in the IKL and the Hubbard model, we find these two models share several common properties around Mott insulator-metal transition as following. (i) A robust NFL state is revealed around the transition with a linear-T resistivity (e.g., Fig. 2f). (ii) The Mott transition is turned out to be third-order, indicated by the divergence of $\frac{\partial^2 n_c}{\partial \mu^2}$. (iii) Resistivity satisfies a quantum critical scaling like Eq. 2 with similar critical exponent $((z\nu)_{\rm IKL}=1.25,(z\nu)_{\rm Hubbard}=1.35)$.

There also exist some differences. The doped MI in the IKL has rigid band while in the Hubbard model spectral-weight transfer leads to non-rigid band. Furthermore, our Monte Carlo simulation in the IKL includes both local and nonlocal correlation, and consequently the low temperature phases of the IKL turn out to be magnetic ordered states. Although

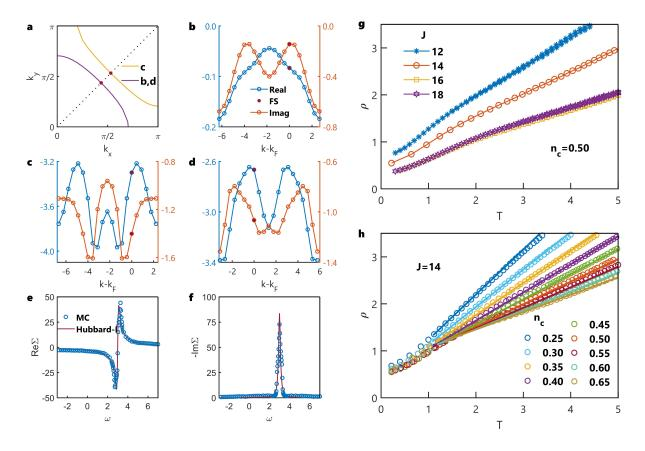


FIG. 4. **NFL-like self-energy and the resultant linear**-T **resistivity. a-d** Momentum dependence to the self-energy calculated around the Fermi energy. **a** Schematic picture for the Fermi surface in **b-d**. In **b** and **d**, Fermi surface (purple line) coincides with each other, whereas the electron density in **b** (FL, IL = 0.72) is double the one in **d** (NFL-II, IL = 0.36). The self-energy is calculated along the black doted line and the position of Fermi surface is marked with red circle. **b-d** Momentum dependence to the self-energy in FL (**b**, J = 2, T = 0.4, $\mu = -0.8$), SM (**c**, J = 14, T = 1, $\mu = -3.0$) and NFL-II (**d**, J = 14, T = 1, $\mu = -4.6$). In FL, the real part of the self-energy demonstrates a linear dependence of momentum, while the imaginary part shows a quadratic dependence, i.e., Re $\Sigma(\omega = 0) \sim k - k_F$ and Im $\Sigma(\omega = 0) \sim (k - k_F)^2$. In contrast, the SM and NFL-II states display a linear momentum dependence for both the real and imaginary parts of self-energy, Re $\Sigma(\omega = 0) \sim k - k_F$ and Im $\Sigma(\omega = 0) \sim k - k_F$. **e-f** Frequency dependence of self-energy in SM ($\mu = -3.0$, T = 1.0). Result of the Hubbard-I approximation valid at strong coupling limit is displayed (red line), and it is in good agreement with MC data (blue circle). **g-h** Robust linear-T resistivity revealed with eq.4 at varying coupling strength within a wide range of doping. **g** Resistivity calculated under fixed doping ($n_C = 0.50$) but varying coupling strength. **h** Resistivity calculated under different doping at fixed coupling strength J = 14. The solid line is fitted by the function $\rho(T, n_C) \approx \rho_0[n_C + \frac{C}{n_C}T]$.

at the absence of QCP, the quantum scaling behavior is confirmed in this solid platform. However, the DMFT applied in the Hubbard model makes a strong approximation such that the magnetic orders are suppressed at low temperature. Considering multiple low-temperature competing orders are all neglected, the uncovered QCP and even the quantum critical behavior in DMFT study might be artificial.

Comparing the IKL to solvable doped MI in the HK model,⁵¹ one see that no Luttinger surface exists in the IKL (also in the SYK and Hubbard) while the HK supports robust Luttinger surface characterized by zeros of Green function. Thus, the Luttinger surface may not be generic feature for doped MI though it does kill FL.

In conclusion, by studying a numerically solvable doped MI, exotic SM behaviors are revealed in the QCR, including the nonsaturating *T*-linear resistivity and the logarithmic

temperature dependence of specific-heat coefficient. These exotic behaviors elucidate the absence of quasiparticle, and it is further confirmed unambiguously by the violation of Luttinger theorem throughout the whole paramagnetic region in the phase diagram. All these SM characteristics all could be traced to an anomalous electron self-energy. The nontrivial formula for self-energy is extracted from the Monte Carlo data, which gives the robust linear-T resistivity and the slope is consistent with the existing experimental data for several materials, e.g., the cuprates, heavy fermion and quantum critical metal $Sr_3Ru_2O_7^{6,\bar{1}0}$, and even the magic-angle graphene⁵⁴. Compared with the classic Hubbard model, our study suggests that SM, Mott quantum criticality and the presence of Fermi surface with NFL-like self-energy are the intrinsic features of doped MI, which are promising to be revealed in generic strongly correlated electron systems.

Methods

Monte Carlo simulations of the IKL are carried out on the square lattice with periodic boundary conditions, where a 20×20 square lattice is mainly used. Accordingly, the two-dimensional Brillouin zone is sampled by a 20×20 k-point grid. Nearest neighbor hopping integral is used as the unit (t=1) to measure all energy scales. To attack the Mottness, we focus on the strong coupling regime (J=14).

ACKNOWLEDGMENTS

This research was supported in part by Supercomputing Center of Lanzhou University and NSFC under Grant No. 11704166, No. 11834005, No. 11874188, No. 11674139. We thank the Supercomputing Center of Lanzhou University for allocation of CPU time.

* zhongy@lzu.edu.cn

- Patrick A. Lee, Naoto Nagaosa, and Xiao-Gang Wen. Doping a mott insulator: Physics of high-temperature superconductivity. *Rev. Mod. Phys.*, 78:17–85, Jan 2006.
- ² G. R. Stewart. Superconductivity in iron compounds. Rev. Mod. Phys., 83:1589–1652, Dec 2011.
- ³ B J Powell and Ross H McKenzie. Quantum frustration in organic mott insulators: from spin liquids to unconventional superconductors. *Reports on Progress in Physics*, 74(5):056501, apr 2011.
- ⁴ Bin Shen, Yongjun Zhang, Yashar Komijani, Michael Nicklas, Robert Borth, An Wang, Ye Chen, Zhiyong Nie, Rui Li, Xin Lu, and et al. Strange-metal behaviour in a pure ferromagnetic kondo lattice. *Nature*, 579(7797):51–55, Mar 2020.
- ⁵ Ramzy Daou, Nicolas Doiron-Leyraud, David LeBoeuf, SY Li, Francis Laliberté, Olivier Cyr-Choiniere, YJ Jo, Luis Balicas, J-Q Yan, J-S Zhou, et al. Linear temperature dependence of resistivity and change in the fermi surface at the pseudogap critical point of a high-t c superconductor. *Nature Physics*, 5(1):31–34, 2009.
- ⁶ A Legros, S Benhabib, W Tabis, F Laliberté, M Dion, M Lizaire, B Vignolle, D Vignolles, H Raffy, ZZ Li, et al. Universal t-linear resistivity and planckian dissipation in overdoped cuprates. *Nature Physics*, 15(2):142–147, 2019.
- ⁷ F Kagawa, K Miyagawa, and K Kanoda. Unconventional critical behaviour in a quasi-two-dimensional organic conductor. *Nature*, 436(7050):534–537, 2005.
- ⁸ H. Oike, K. Miyagawa, H. Taniguchi, and K. Kanoda. Pressure-induced mott transition in an organic superconductor with a finite doping level. *Phys. Rev. Lett.*, 114:067002, Feb 2015.
- ⁹ S. S. P. Parkin, E. M. Engler, R. R. Schumaker, R. Lagier, V. Y. Lee, J. C. Scott, and R. L. Greene. Superconductivity in a new family of organic conductors. *Phys. Rev. Lett.*, 50:270–273, Jan 1983
- JAN Bruin, H Sakai, RS Perry, and AP Mackenzie. Similarity of scattering rates in metals showing t-linear resistivity. *Science*, 339(6121):804–807, 2013.
- ¹¹ Jan Zaanen. Planckian dissipation, minimal viscosity and the transport in cuprate strange metals. *SciPost Phys.*, 6:61, 2019.
- Bernhard Keimer, Steven A Kivelson, Michael R Norman, Shinichi Uchida, and J Zaanen. From quantum matter to high-temperature superconductivity in copper oxides. *Nature*, 518(7538):179–186, 2015.
- J Custers, Philipp Gegenwart, H Wilhelm, K Neumaier, Y Tokiwa, O Trovarelli, C Geibel, F Steglich, C Pépin, and Piers Coleman. The break-up of heavy electrons at a quantum critical point. *Nature*, 424(6948):524–527, 2003.
- P. W. ANDERSON. The resonating valence bond state in la2cuo4 and superconductivity. *Science*, 235(4793):1196–1198, 1987.
- ¹⁵ Ian Affleck, Z. Zou, T. Hsu, and P. W. Anderson. Su(2) gauge symmetry of the large-u limit of the hubbard model. *Phys. Rev.* B, 38:745–747, Jul 1988.
- ¹⁶ Xiao-Gang Wen and Patrick A. Lee. Theory of underdoped

- cuprates. Phys. Rev. Lett., 76:503-506, Jan 1996.
- J. Vučičević, D. Tanasković, M. J. Rozenberg, and V. Dobrosavljević. Bad-metal behavior reveals mott quantum criticality in doped hubbard models. *Phys. Rev. Lett.*, 114:246402, Jun 2015.
- J. Vučičević, H. Terletska, D. Tanasković, and V. Dobrosavljević. Finite-temperature crossover and the quantum widom line near the mott transition. *Phys. Rev. B*, 88:075143, Aug 2013.
- ¹⁹ L. D. Landau. The theory of a Fermi liquid. Sov. Phys., JETP, 3:920–925, 1957.
- ²⁰ Ian Osborne, Thereza Paiva, and Nandini Trivedi. Fermi-surface reconstruction in the repulsive fermi-hubbard model, 2020.
- Edwin W Huang, Ryan Sheppard, Brian Moritz, and Thomas P Devereaux. Strange metallicity in the doped hubbard model. *Science*, 366(6468):987–990, 2019.
- Antoine Georges, Gabriel Kotliar, Werner Krauth, and Marcelo J. Rozenberg. Dynamical mean-field theory of strongly correlated fermion systems and the limit of infinite dimensions. *Rev. Mod. Phys.*, 68:13–125, Jan 1996.
- ²³ G. Kotliar, S. Y. Savrasov, K. Haule, V. S. Oudovenko, O. Parcollet, and C. A. Marianetti. Electronic structure calculations with dynamical mean-field theory. *Rev. Mod. Phys.*, 78:865–951, Aug 2006
- P Limelette, A Georges, D Jérome, P Wzietek, P Metcalf, and JM Honig. Universality and critical behavior at the mott transition. *Science*, 302(5642):89–92, 2003.
- S. Tsuda, C. L. Yang, Y. Shimura, K. Umeo, H. Fukuoka, Y. Yamane, T. Onimaru, T. Takabatake, N. Kikugawa, T. Terashima, H. T. Hirose, S. Uji, S. Kittaka, and T. Sakakibara. Metamagnetic crossover in the quasikagome ising kondo-lattice compound ceirsn. *Phys. Rev. B*, 98:155147, Oct 2018.
- ²⁶ John Shin, Zack Schlesinger, and B. Sriram Shastry. Kondo-ising and tight-binding models for tmb₄. *Phys. Rev. B*, 95:205140, May 2017.
- A. E. Sikkema, W. J. L. Buyers, I. Affleck, and J. Gan. Ising-kondo lattice with transverse field: A possible f-moment hamiltonian for uru₂si₂. *Phys. Rev. B*, 54:9322–9327, Oct 1996.
- Wei-Wei Yang, Jize Zhao, Hong-Gang Luo, and Yin Zhong. Exactly solvable kondo lattice model in the anisotropic limit. *Phys. Rev. B*, 100:045148, Jul 2019.
- 29 See the detail of Monte Carlo simulation in Supplementary Materials
- 30 See Supplementary Materials for low-T magnetic states. The magnetic-paramagnetic phase transition (Fig. 2b, purple line with circle) is determined by the peak in heat capacity (see Fig. 2d) and belongs to the two-dimensional Ising universality class, which is similar to the half-filled IKL.
- See $n_c T$ phase diagram in Supplementary Materials.
- 32 Chandra M Varma. Quantum-critical fluctuations in 2d metals: strange metals and superconductivity in antiferromagnets and in cuprates. Reports on Progress in Physics, 79(8):082501, jul 2016.
- ³³ Chandra M. Varma. Colloquium: Linear in temperature resistivity

- and associated mysteries including high temperature superconductivity. Rev. Mod. Phys., 92:031001, Jul 2020.
- ³⁴ Ian M Hayes, Ross D McDonald, Nicholas P Breznay, Toni Helm, Philip JW Moll, Mark Wartenbe, Arkady Shekhter, and James G Analytis. Scaling between magnetic field and temperature in the high-temperature superconductor bafe 2 (as 1- x p x) 2. *Nature Physics*, 12(10):916–919, 2016.
- ³⁵ C. M. Varma, P. B. Littlewood, S. Schmitt-Rink, E. Abrahams, and A. E. Ruckenstein. Phenomenology of the normal state of cu-o high-temperature superconductors. *Phys. Rev. Lett.*, 63:1996– 1999, Oct 1989.
- ³⁶ Steven A Kivelson, Eduardo Fradkin, and Victor J Emery. Electronic liquid-crystal phases of a doped mott insulator. *Nature*, 393(6685):550–553, 1998.
- ³⁷ Dirk Van Der Marel, HJA Molegraaf, J Zaanen, Z Nussinov, Fabrizio Carbone, A Damascelli, H Eisaki, M Greven, PH Kes, and M Li. Quantum critical behaviour in a high-t c superconductor. *Nature*, 425(6955):271–274, 2003.
- ³⁸ Jan Zaanen. Why the temperature is high. *Nature*, 430(6999):512–513, 2004.
- 39 These results are crosschecked by a DMFT study in Supplementary Materials. Out of QCR, we dub the NFL state without quantum scaling behavior as the second non-Fermi liquid (NFL-II). The characteristics of NFL-I and NFL-II are demonstrated in detail in the supplementary materials.
- In this paper we determine the separatrix by the minimum of error bar with varying doping at a specific temperature in Monte Carlo simulation, see details in the supplementary materials.
- Out of QCR, we dub the NFL state without quantum scaling behavior as the second non-Fermi liquid (NFL-II). The characteristics of NFL-I and NFL-II are demonstrated in detail in the supplementary materials.
- ⁴² The critical exponent for c electron $((zv)_c = 1.25)$ is different from the one of f electron $((zv)_f = 0.55)$.

- ⁴³ Igor Dzyaloshinskii. Some consequences of the luttinger theorem: The luttinger surfaces in non-fermi liquids and mott insulators. *Phys. Rev. B*, 68:085113, Aug 2003.
- ⁴⁴ J. M. Luttinger. Fermi surface and some simple equilibrium properties of a system of interacting fermions. *Phys. Rev.*, 119:1153–1163, Aug 1960.
- Masaki Oshikawa. Topological approach to luttinger's theorem and the fermi surface of a kondo lattice. *Phys. Rev. Lett.*, 84:3370– 3373, Apr 2000.
- 46 See details of the analytic Hubbard-I approximation in the supplementary materials.
- ⁴⁷ Max A. Metlitski and Subir Sachdev. Quantum phase transitions of metals in two spatial dimensions. i. ising-nematic order. *Phys. Rev. B*, 82:075127, Aug 2010.
- ⁴⁸ Max A. Metlitski and Subir Sachdev. Quantum phase transitions of metals in two spatial dimensions. ii. spin density wave order. *Phys. Rev. B*, 82:075128, Aug 2010.
- ⁴⁹ Alexei Kitaev. A simple model of quantum holography. In *KITP* strings seminar and Entanglement, volume 12, page 26, 2015.
- ⁵⁰ Juan Maldacena and Douglas Stanford. Remarks on the sachdevye-kitaev model. *Phys. Rev. D*, 94:106002, Nov 2016.
- ⁵¹ Philip W. Phillips, Luke Yeo, and Edwin W. Huang. Exact theory for superconductivity in a doped mott insulator. *Nature Physics*, Jul 2020.
- Peter Cha, Aavishkar A. Patel, Emanuel Gull, and Eun-Ah Kim.
 Slope invariant *t*-linear resistivity from local self-energy. *Phys. Rev. Research*, 2:033434, Sep 2020.
- ⁵³ See the fitting coefficient a and Γ under different coupling strength in the supplementary materials.
- Yuan Cao, Debanjan Chowdhury, Daniel Rodan-Legrain, Oriol Rubies-Bigorda, Kenji Watanabe, Takashi Taniguchi, T. Senthil, and Pablo Jarillo-Herrero. Strange metal in magic-angle graphene with near planckian dissipation. *Phys. Rev. Lett.*, 124:076801, Feb 2020.